# 3D Sensing Framework for Outdoor Navigation

**Roman Katz, Narek Melkumyan, Jose Guivant, Tim Bailey and Eduardo Nebot**
ARC Centre of Excellence for Autonomous Systems
Australian Centre for Field Robotics
The University of Sydney, Australia
{r.katz}@cas.edu.au

## Abstract

Although full 3D navigation and mapping is recognized as one of the most important challenges for autonomous navigation, the lack of robust sensors, providing 3D information in real time, has burdened the progress in this direction. This paper presents our ongoing work towards the deployment of a 3D sensory system for environmental sensing in outdoor environments. We first describe a 3D data acquisition architecture based on a standard 2D laser. Techniques for registering scans using a scan matching procedure and for estimating the errors are then introduced. We also present results showing the performance of the architecture in real outdoor environments, and discuss further improvements of the proposed architecture.

## 1 Introduction

Environment sensing is a core problem in the design of autonomous mobile robots. A crucial part of the performance of a robot highly depends on the accuracy and reliability of what it perceives [Nuchter *et al.*, 2005] and how it processes and interprets the sensory information. A sound and precise environmental representation is actually required for several different purposes: localisation, path planning, detection of particular properties in the environment [Lacroix *et al.*, 2002].

In the past few years significant work has been carried out in navigation and simultaneous localization and mapping (SLAM) [Leonard and Durrant-Whyte, 1991; Dissanayake *et al.*, 2001]. The vehicle position is evaluated by combining the data received from the internal sensors such as encoders and external sensors such as lasers, radar or GPS. Laser has become very popular in SLAM applications [Henriksen and Krotkov, 1997; Thrun *et al.*, 2000; Guivant and Nebot, 2001]. Although this sensor is able to obtain 2D range and bearing scans of the environment fast and accurately, for many 2D navigation applications –specially in outdoor environments– this might not provide enough information. Full 3D navigation and mapping in unstructured all terrain environments is recognized, in fact, as on of the most important challenges for autonomous navigation. The lack of robust sensors capable of providing rich 3D information in real time has been one of the main limiting factors in this sense.

Sensory procedures in indoor environments are usually simplified since the complexity of the problem can be reduced by assuming flat floors and well defined and crisp geometry (determined by the interior of rooms and corridors). Within this setup, the utilization of 2D laser range scanner appears to be sufficient for purposes of robot mapping and sensor based navigation. However, outdoor environments present very different challenges from indoor environments. The irregular nature of the non-flat outdoor terrain prevents the immediate use of 2D laser scans when the robot is rolling and pitching [Cole *et al.*, 2005]. Moreover, the complexity of the obstacles (e.g., trees, rocks, bush, cars, etc.) usually requires more robust, probably 3D sensory approaches. This is why, in order to achieve real autonomy in outdoor environments, we need to rely on more complex sensory mechanisms, such as the one provided by a 3D laser range scanner.

In this work we discuss our progress towards the deployment of a 3D sensory system for environmental sensing and navigation in outdoor environments. The developed 3D data acquisition architecture is first introduced and described in detail in Section 2. The 3D laser range scanner is built on the basis of a standard 2D laser by extension with a mount and a servo motor, such that it can robustly capture the distance to surface points on 3D objects within long ranges.

It is clear that, for almost any autonomous task, the robot must know its position within the environment. Dead reckoning sensors generate an unbounded error that needs to be compensated to obtain a more accurate

estimate of the robot position. One way to achieve this is to match range scans [Bailey, 2002] taken at different locations at different times in the environment, and to update the position estimation according to the matching result. Moreover, an accurate registration procedure to assemble 3D scans into one consistent global representation is useful for mapping. Therefore, Section 3 presents the basic concepts for the registration of the 3D scans obtained with the 3D laser range scanner described in Section 2.

Some information about the uncertainty of the registration is probably as important as an accurate registration method. In fact, an estimation of the registration errors can provide a valuable measure of the accuracy of the scan matching procedure. This becomes particularly relevant in outdoor environments, where difficult setting configuration (long walls, corridors, repetitive patterns such as trees or cars, etc.) might "confuse" the registration procedure and lead to a high uncertain alignment. Moreover, the uncertainty of the registration –preferably in the form of a covariance matrix– is mandatory if we want to use the estimated 3D registration pose in a probabilistic framework (such as a Kalman filter) with information provided by other sensors. The approach proposed in [Bengtsson and Baerveldt, 2003] for the estimation of the registration errors is then described in Section 4.

Some experimental results of the 3D data acquisition architecture are presented in Section 5. We illustrate the performance of the system by showing images of the obtained 3D scans taken in real world outdoor environment, together with both the 3D registration poses and the corresponding estimation of the registration errors. Conclusions and future work are finally discussed in Section 6.

## 2 Description of the 3D Data Acquisition Architecture

We have developed a 3D data acquisition architecture built on the basis of a 2D Sick LMS-200 [Sick, 2005] laser scanner and an Amtec PowerCube PR090 servo motor. The images in Figure 2 show the 3D laser scanner, together with images of the system mounted on top of the research vehicle and the 3D coordinate frame.

The Sick LMS-200 laser scanner can obtain a 180 degree scan of the environment in 13 and 26 msec with 1 and 0.5 degree resolution respectively. The maximum range of the 3D scanner is approximately 80m with 1 cm resolution. In order to achieve high data rates a dedicated hardware/software system is required to read the data at 500Kb through a RS422 interface. The additional servo system required to scan in the other dimension has the following main technical characteristics: nominal R.P.M: 4300 m-1, encoder resolution: 2000 inc/rotation and maximal angular velocity: 238°/sec. The data is transferred in real time via serial interface RS232 at 38400 bps.

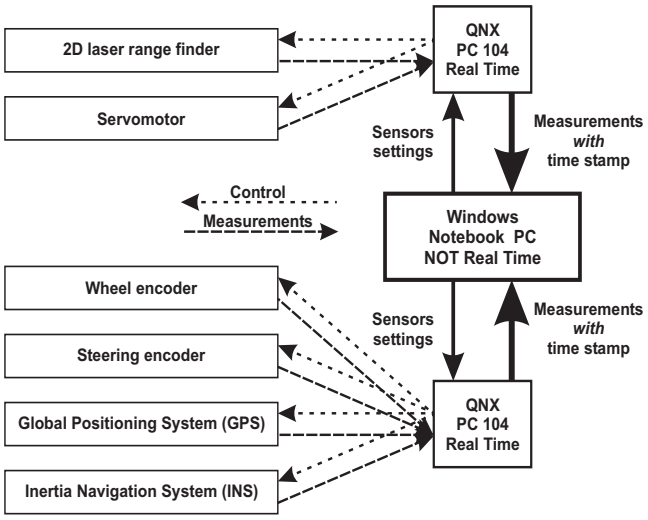


Figure 1: Image showing the 3D scanner embedded in the general sensing architecture of the research vehicle.

The control of the 3D scanner system is done with a dedicated PC104 system running under QNX operating system [QNX, 2005]. A standard Xtreme/104 Opto board with 8Mhz oscillator is used to get the non standard serial speed of (500000bps). The sensor system can be programmed by the user in order to scan with a selected resolution, speed, and angle span. It then broadcasts raw laser/orientation data with the appropriate time-stamps through a standard ethernet interface. With this mechanism a client can be written to use this data using any other operating system. The same approach is used to acquire data and time-stamp from the other sensors in the research vehicle. The diagram of the 3D scanner embedded in the general sensing architecture of the research vehicle is shown in Figure 1. [1]

In this way very accurate time-stamped data is obtained with front end processors using efficient hard real time systems. The information is then broadcasted to the client that can process the information in almost real time. This is an important concept since most of the other processes such as scan matching, path planning, etc., are not as time critical as data acquisition. Hence, we can use hard real time systems only where is needed most, and implement the high level tasks in other operating system where we have additional debugging and display facilities.

[1] In fact, the research vehicle system is retrofitted with velocity and steering encoders, a full six degree of freedom Inertial Measurement Unit and GPS.


(a) (b) (c)

Figure 2: Images showing the 3D data acquisition architecture. 3D laser range scanner in (a), system mounted on the research vehicle in (b), and coordinate frame of the 3D system in (c).

## 3 3D Registration using Scan Matching

In this section we present the basic concepts for registation of 3D scans. Let $P = \{\mathbf{b}_i\}$ be a measurement data point set containing $N_b$ 3D points, and a model point set $X = \{\mathbf{a}_i\}$ considered fixed and containing $N_a$ 3D points. The goal of the registration is to find a transformation vector to align the data points of $P$ to the model points of $X$. This transformation is composed by a 3D translation and rotation, such that it can be characterized by the six parameter vector $\mathbf{z} = [x, y, z, \alpha, \beta, \gamma]^T$.

In general, the general error metric to be minimized takes the form:

$$E(\mathbf{z}) = \sum_{i=1}^{N_b} \|\mathbf{a}_i - (\mathbf{R}\mathbf{b}_i + \mathbf{T})\|^2, \qquad (1)$$

where each of the $\mathbf{b}_i$ in the measurement data points ($N_b$) corresponds to the nearest point $\mathbf{a}_i$ in the model set, $\mathbf{R}$ is the rotation matrix and $\mathbf{T}$ is the translation vector, these two ($\mathbf{R}$,$\mathbf{T}$) defining the registration vector $\mathbf{z} = [x, y, z, \alpha, \beta, \gamma]^T$.

Instead of calculating the transformation ($\mathbf{R}$,$\mathbf{T}$) directly in the original parameter space $\mathbf{z}$ it is convenient to use the quaternion based method presented in [Horn, 1987], where the transformation is expressed in terms of the vector $\mathbf{q} = [q_0, q_1, q_2, q_3, q_4, q_5, q_6]^T$. The unit quaternion is a four vector $\mathbf{q_R} = [q_0, q_1, q_2, q_3]^T$, where $q_0 \geq 0$, and $q_0^2 + q_1^2 + q_2^2 + q_3^2 = 1$. The $3 \times 3$ rotation matrix $\mathbf{R}$ generated by a unit quaternion is then calculated according to the following scheme:

$$\mathbf{R} = \begin{bmatrix} r_{11} & r_{12} & r_{13} \\ r_{21} & r_{22} & r_{23} \\ r_{31} & r_{32} & r_{33} \end{bmatrix}, \qquad (2)$$

with:

$$\begin{aligned} r_{11} &= q_0^2 + q_1^2 - q_2^2 - q_3^2 \\ r_{12} &= 2(q_1 q_2 - q_0 q_3) \\ r_{13} &= 2(q_1 q_3 + q_0 q_2) \\ r_{21} &= 2(q_1 q_2 + q_0 q_3) \\ r_{22} &= q_0^2 + q_2^2 - q_1^2 - q_3^2 \\ r_{23} &= 2(q_2 q_3 - q_0 q_1) \\ r_{31} &= 2(q_1 q_3 - q_0 q_2) \\ r_{32} &= 2(q_2 q_3 + q_0 q_1) \\ r_{33} &= q_0^2 + q_3^2 - q_1^2 - q_2^2. \end{aligned}$$

If this rotation is characterized by $Z-Y-X$ Euler angles, the three angles $[\alpha, \beta, \gamma]$ can be obtained as follows:

$$\begin{aligned} \alpha &= atan2(r_{21}/\cos\beta, r_{11}/\cos\beta) \\ \beta &= atan2(-r_{31}, \sqrt{r_{11}^2 + r_{21}^2}) \\ \gamma &= atan2(r_{32}/\cos\beta, r_{33}/\cos\beta). \end{aligned} \qquad (3)$$

The translation $\mathbf{T}$ is given by the vector:

$$\mathbf{T} = [x, y, z]^T = [q_4, q_5, q_6]^T. \qquad (4)$$

The ICP algorithm can be stated as in [Besl and McKay, 1992; Bailey, 2002] as follows:

- The data point set $P$ with $N_b$ points $\mathbf{b_i}$ and the model point set $X$ with $N_a$ points $\mathbf{a_i}$ are given.
- The iteration is initialized by setting an initial pose $\mathbf{q}_0 = [1, 0, 0, 0, 0, 0, 0]^T$, $P = P_0$ and $k = 0$. The registration vectors are defined relative to the initial data set $P_0$ so that the final registration represents the complete transformation. The next three steps 1, 2 and 3 are repeated until convergence within certain tolerance (determined by a least-mean-squared

residual threshold), or indicated by a fixed number of iterations.

1. Each point $\mathbf{b}_i$ in $P_0$ is transformed to $P_k = \{\mathbf{R}\mathbf{b}_i + \mathbf{T}\}$ using the current pose estimate $\mathbf{q}_k$ and the expressions in (2) and (4).
2. Each transformed point in $P_k$ is associated to its nearest neighbor in $X$.
3. The associated pairs are used to calculate the relative pose $\mathbf{q}_{k+1}$ that minimizes the least-mean-squared error (1) between the associated points.

The final registration transformation is obtained upon convergence from $\mathbf{q}_{k+1}$ using (2)-(4).

## 4 Estimation of the Registration Errors

In general not only an accurate matching is important, but also a sound measure of the quality of the matching, i.e., the accuracy of the estimated 3D pose. This is specially important if we want to fuse the estimated 3D registration pose with information from other sources in a multi-sensor probabilistic framework (e.g., a Kalman filter).

As illustrated in [Bengtsson and Baerveldt, 2003], the approach taken in [Lu and Milios, 1997] shows how a covariance matrix can be estimated directly from the corresponding pair of points. This estimation is based on the assumption that the algorithm always finds the same physical point in the measurement data point set and the model point set. This assumption can be easily violated when the environment lacks of complex structure or when it contains repetitive patterns. A simple setting example is that of a robot moving in a long corridor: the corresponding pairs of points do not necessarily represent the same physical points in two scans, because the scans can be taken indistinctly at any location along the corridor. The result given by [Lu and Milios, 1997] is much too optimistic in the direction along the corridor. Even though the alignment provides enough information to produce an accurate alignment in the direction perpendicular to the corridor walls, the uncertainty in the direction along the walls should be large (it should tend to infinite if considering ideal infinite walls).

We choose for the estimation of the registration error the approach described in [Bengtsson and Baerveldt, 2003] This procedure considers the uncertainty given by the environment layout and thus provides a more accurate estimation for the covariance matrix. Its basic concepts are more easily described if we rewrite (1) as:

$$E(\mathbf{z}) = (\mathbf{A} - M\mathbf{z})^T(\mathbf{A} - M\mathbf{z}), \tag{5}$$

where $\mathbf{A}$ contains the model points $\mathbf{a}_i$, $M$ is the observation matrix, and $\mathbf{z}$ is the registration vector. The observation matrix $M$ ([Xiong and Wang, 2004; Wang, 2000]) is defined to relate errors in the transformation parameters to dimensional errors of the measurement point, as follows:

$$\epsilon = M\delta\mathbf{t},$$

with $\epsilon = [\epsilon_1, \epsilon_2, \ldots, \epsilon_{N_b}]^T$ the vector containing the dimensional errors, $\delta\mathbf{t} = [\delta t_1, \delta t_2, \delta t_3, \delta t_4, \delta t_5, \delta t_6]^T$ the vector containing the errors in each transformation parameter, and $M$ defined as in [Menq *et al.*, 1992] as:

$$M = \begin{bmatrix} n_1^x & n_1^y & n_1^z & -(\mathbf{n}_1 \times \mathbf{b}_1)^T \\ n_2^x & n_2^y & n_2^z & -(\mathbf{n}_2 \times \mathbf{b}_2)^T \\ \ldots & \ldots & \ldots & \ldots \\ n_{N_b}^x & n_{N_b}^y & n_{N_b}^z & -(\mathbf{n}_{N_b} \times \mathbf{b}_{N_b})^T \end{bmatrix}, \tag{6}$$

with $\mathbf{b}_i$ the $i^{th}$ measurement point and $\mathbf{n}_i = [n_i^x, n_i^y, n_i^z]^T$ the normal vector at the $i^{th}$ measurement point.

The optimal state of (5) for the parameter vector $\mathbf{z}$ and $cov(\mathbf{z})$ are according to [Kay, 1993] as follows:

$$\mathbf{z} = (M^T M)^{-1} M^T A \tag{7}$$

$$cov(\mathbf{z}) = (M^T M)^{-1}\sigma^2 \tag{8}$$

An unbiased estimate of $\sigma^2$ can be calculated as:

$$\hat{\sigma}^2 = \frac{\hat{E}(\mathbf{z})}{n - k - 1} \tag{9}$$

where $\hat{E}(\mathbf{z})$ is the minimized error for (5) at the found registration vector $\mathbf{z}$, $n$ is the number of point matches of the registration and $k$ is the number of estimated parameters.

A double differentiation of (5) gives the Hessian matrix H, as:

$$H = \frac{dE^2(\mathbf{z})}{d\mathbf{z}^2} = 2M^T M \Rightarrow M^T M = \frac{1}{2}H. \tag{10}$$

Then, by combining (8), (9) and (10) the covariance $cov(\mathbf{z})$ becomes:

$$cov(\mathbf{z}) = \left(\frac{1}{2}H\right)^{-1}\hat{\sigma}^2. \tag{11}$$

Once the scan matching algorithm has found the registration vector $\mathbf{z}$, each of the elements in the Hessian matrix $H$ can be estimated. It is clear that for the case of a complete 3D registration with $\mathbf{z} = [x, y, z, \alpha, \beta, \gamma]^T$, the Hessian $H$ is a $6\times6$ matrix, with the components corresponding to the second order partial derivatives. The calculation of the elements of $H$ is done by first translating and rotating the measurement data point set of the actual scan; and then letting the registration algorithm find again the corresponding pair of points for the transformation, now affected by small perturbations in each

of the parameters of the registration. In other words, the elements of the Hessian matrix H are calculated as follows:

1. Translate and rotate the measurement data point set of the actual scan according to the found registration vector $\mathbf{z}$ plus a small perturbation $\delta\mathbf{z} = [\delta x, \delta y, \delta z, \delta\alpha, \delta\beta, \delta\gamma]^T$.
2. Find the new corresponding pair of points in the model set point and in the modified transformed measurement data point set of the actual scan.
3. Calculate (5) based on the new corresponding pairs of points.
4. Repeat steps 1-3 until all elements of the Hessian matrix $H$ are calculated.

The second order partial derivatives for the Hessian matrix $H$ are calculated as exemplified below for $\frac{\partial^2 E}{\partial x \partial y}$:

$$\frac{\partial^2 E}{\partial x \partial y} \approx \frac{\frac{E(\mathbf{z}+\Delta x+\Delta y)-E(\mathbf{z}-\Delta x+\Delta y)}{4\Delta x\Delta y} - \frac{E(\mathbf{z}+\Delta x-\Delta y)-E(\mathbf{z}-\Delta x-\Delta y)}{4\Delta x\Delta y}}{} \quad (12)$$

for some given values of $\Delta x$ and $\Delta y$.

## 5 Experimental Evaluation

In this section we present experimental results showing the performance of the 3D data acquisition system in outdoor environments.

The images shown in Figure 3 present scans taken in the outdoor area near the ACFR building using the system described in Section 2. The vehicle moved along the area, stopping every several meters and taking full 3D scans in each of these stops. As can be appreciated from the images, the scans contain a large amount of information, clearly delineating the environment structure and its obstacles, even in long ranges.

Figure 4 presents the aligned scans resulting from the 3D registration using the scan matching procedure described in Section 3. Each of the images in Figure 4 corresponds to aligned pairs in Figure 3: 4(a) to 3(a)-(b), 4(b) to 3(b)-(c), 4(c) to 3(c)-(d) and 4(d) to 3(d)-(e). Each of the images shows one reference scan together with the superimposed transformed scan (using the registration vector) that corresponds to the next scan in the sequence. Table 1 shows the registration information for the aligned scans of Figure 4. For each pair of aligned scans, the corresponding translation vector, rotation matrix and covariance matrix (for the $x$, $y$ and $z$ parameters) are displayed.

## 6 Conclusions and Future Work

This paper presented the deployed sensory system for 3D environmental sensing in outdoor environments. The 3D data acquisition architecture was described, and techniques for the registration of 3D scans and for the estimation of their errors were analyzed. As illustrated through experiments, the system performs robustly and accurately in real outdoor environments, providing scans of good quality that can be assembled into larger maps consistently.

The possibility of estimating the covariance of the registration permits the use of the 3D registration pose in a probabilistic framework. This is, in fact, a future direction of research, that aims to expand the Scan-SLAM architecture proposed in [Nieto *et al.*, 2005] to 3D mapping representations. We are currently further improving our architecture in two directions. Firstly, we are extending the system to a dynamic scanning framework, in order to be able to fuse scans taken with the moving vehicle. And secondly, we are integrating the 3D laser range finder with a camera, augmenting to 3D the concept presented in [Zhang and Pless, 2004] for 2D.

## 7 Acknowledgments

This work is supported by the CRCMining, the Australian Research Council (ARC) Centre of Excellence program and the New South Wales Government. Also special thanks to QSSL for donating copies of the QNX Momentics Professional development system used to implement the real-time data acquisition system.

## References

[Bailey, 2002] T. Bailey. Mobile Robot Localisation and Mapping in Extensive Outdoor Environments. PhD thesis, University of Sydney, Australia, 2002.

[Bengtsson and Baerveldt, 2003] O. Bengtsson and A-J. Baerveldt. Robot Localization based on Scan–matching – Estimating the Covariance Matrix for the IDC Algorithm. *Robotics and Autonomous Systems*, 44(1):29–40, 2003.

[Besl and McKay, 1992] P. Besl and N. McKay. A Method for Registration of 3-D Shapes. *IEEE Transactions on Pattern Analysis and Machine Intelligence*, 14(2):239–256, 1992.

[Cole *et al.*, 2005] D. Cole, A. Harrison, and P. Newman. Using Naturally Salient Regions for SLAM with 3D Laser Data. In *International Conference on Robotics and Automation, SLAM Workshop*, Barcelona, Spain, 2005. IEEE.

[Dissanayake *et al.*, 2001] M. Dissanayake, P. Newman, S. Clark, H. Durrant-Whyte, and M. Csorba. A Solution to the Simultaneous Localisation and Map Building (SLAM) Problem. *IEEE Transactions on Robotics and Automation*, 17(3):229–241, 2001.

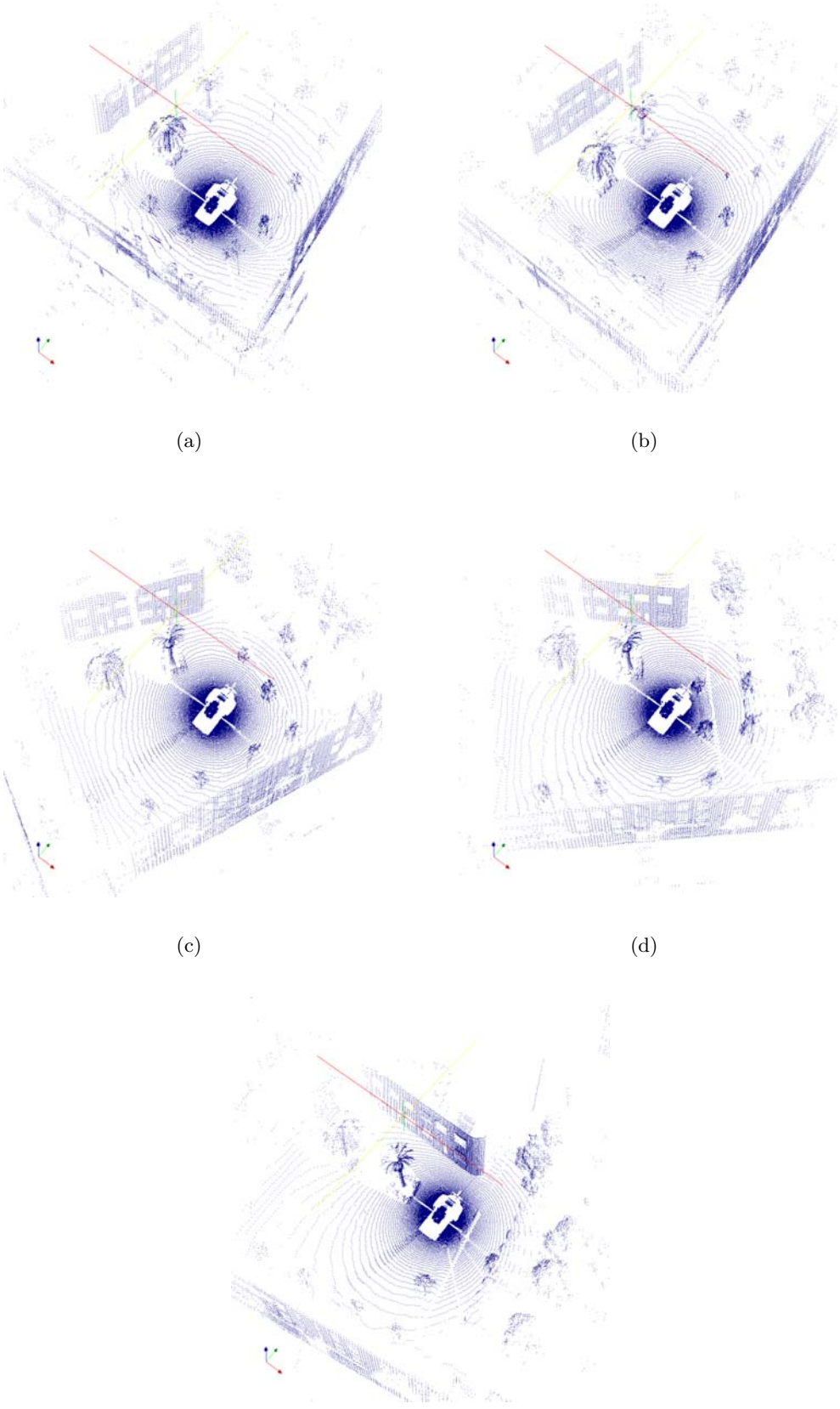

(a) (b)

(c) (d)

(e)

Figure 3: Images showing scans taken in an outdoor setting using the 3D data acquisition system presented in Section 2.

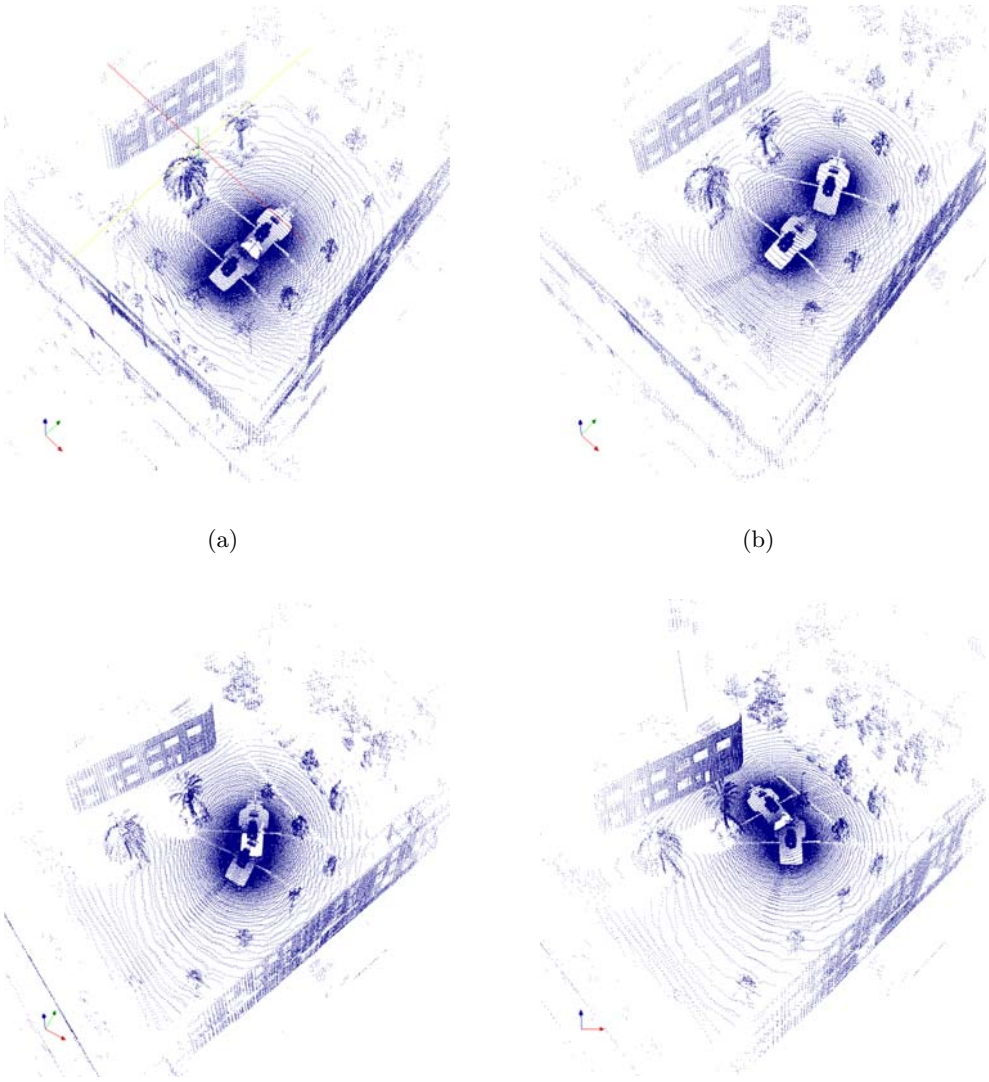

(a) (b)

(c) (d)

Figure 4: Images showing the results of the 3D registration using scan matching. Each of the images shows one reference scan together with the superimposed transformed scan (using the registration vector) that corresponds to the next scan for the sequence in Figure 3.


[Guivant and Nebot, 2001] J. E. Guivant and E. M. Nebot. Optimization of the Simultaneous Localization and Map-building Algorithm for Real-time Implementation. *IEEE Transactions on Robotics and Automation*, 17(3):242–257, 2001.

[Henriksen and Krotkov, 1997] L. Henriksen and E. Krotkov. Natural terrain hazard detection with a laser rangefinder. In *International Conference on Robotics and Automation*, New Mexico, 1997. IEEE.

[Horn, 1987] B. Horn. Closed-form Solution of Absolute Orientation using Unit Quaternions. *Journal of the Optical Society of America A*, 4(4):629–642, 1987.

[Kay, 1993] S. M. Kay. *Fundamentals of Statistical Signal Processing – Estimation Theory*. Prentice–Hall, New Jersey, 1993.

[Lacroix *et al.*, 2002] S. Lacroix, A. Mallet, D. Bonnafous, G. Bauzil, S. Fleury, M. Herrb, and R. Chatila. Autonomous rover navigation in a unknown terrains: Functions and integrations. *The International Journal of Robotics Research*, 21(10):917–942, 2002.

[Leonard and Durrant-Whyte, 1991] J. J. Leonard and H. F. Durrant-Whyte. Simultaneous Map Building

Table 1: Registration information (all units in cms.) for the aligned scans shown in Figure 4.

| Aligned Scans | Translation | Rotation | Covariance |
|---|---|---|---|
| 3(a)-(b)/4(a) | $[-21.9847, 709.6596, -9.6812]^T$ | $\begin{bmatrix} 0.9996 & -0.0292 & 0.0026 \\ 0.0292 & 0.9996 & -0.0056 \\ -0.0024 & 0.0056 & 1.0000 \end{bmatrix}$ | $\begin{bmatrix} 0.1302 & 0.0027 & 0.0260 \\ 0.0027 & 0.9629 & 0.0806 \\ 0.0260 & 0.0806 & 0.1227 \end{bmatrix}$ |
| 3(b)-(c)/4(b) | $[112.6, 1041.2, -24.7]^T$ | $\begin{bmatrix} 0.9033 & -0.4288 & -0.0149 \\ 0.4290 & 0.9030 & 0.0242 \\ 0.0030 & -0.0283 & 0.9996 \end{bmatrix}$ | $\begin{bmatrix} -0.2092 & -0.6897 & -0.3206 \\ -0.6897 & 2.3219 & -0.0786 \\ -0.3206 & -0.0786 & 0.3951 \end{bmatrix}$ |
| 3(c)-(d)/4(c) | $[-105.6955, 449.3803, -5.7095]^T$ | $\begin{bmatrix} 0.9194 & -0.3932 & -0.0063 \\ 0.3933 & 0.9194 & 0.0049 \\ 0.0039 & -0.0069 & 1.0000 \end{bmatrix}$ | $\begin{bmatrix} -2.0494 & -0.8545 & -0.4933 \\ -0.8545 & -0.3242 & 0.0371 \\ -0.4933 & 0.0371 & 0.2708 \end{bmatrix}$ |
| 3(d)-(e)/4(d) | $[-321.8118, 636.9756, -20.2317]^T$ | $\begin{bmatrix} 0.8402 & -0.5419 & -0.0203 \\ 0.5422 & 0.8386 & 0.0522 \\ -0.0113 & -0.0549 & 0.9984 \end{bmatrix}$ | $\begin{bmatrix} 11.3466 & 4.8985 & 0.0609 \\ 4.8985 & 3.3926 & -0.0097 \\ 0.0609 & -0.0097 & 0.5240 \end{bmatrix}$ |


and Localization for an Autonomous Mobile Robot. In *IEEE/RSJ International Workshop on Intelligent Robots and Systems*, Osaka, Japan, 1991. IEEE.

[Lu and Milios, 1997] F. Lu and E. Milios. Robot Pose Estimation in Unknown Environments by Matching 2D Range Scans. *Journal of Intelligent and Robotic Systems*, 18:249–275, 1997.

[Menq *et al.*, 1992] C. H. Menq, H. T. Yau, and G. Y. Lai. Automated Precision Measurement of Surface Profile in CAD Directed Inspection. *IEEE Transactions on Robotics and Automation*, 8(2):268–278, 1992.

[Nieto *et al.*, 2005] J. Nieto, T. Bailey, and E. Nebot. Scan-SLAM: Combining EKF-SLAM and Scan Correlation. In *International Conference on Robotics and Automation, SLAM Workshop*, Barcelona, Spain, 2005. IEEE.

[Nuchter *et al.*, 2005] A. Nuchter, K. Lingemann, J. Hertzberg, and H. Surmann. Accurate Object Localization in 3D Laser Range Scans. In *12th International Conference on Advanced Robotics*, Seattle, USA, 2005. IEEE.

[QNX, 2005] QNX. QNX Programmer's Guide, 2005.

[Sick, 2005] Sick. Sick Laser Data Sheets, 2005.

[Thrun *et al.*, 2000] S. Thrun, W. Burgard, and D. Fox. A real-time algorithm for mobile robot mapping with application to multi-robot and 3D mapping. In *International Conference on Robotics and Automation*, San Francisco, California, 2000. IEEE.

[Wang, 2000] M. Y. Wang. An Optimum Design for 3D Fixture Synthesis in a Point Set Domain. *IEEE Transactions on Robotics and Automation*, 16(6):839–846, 2000.

[Xiong and Wang, 2004] Z. Xiong and M. Y. Wang. A Near–Optimal Probing Strategy for Workpiece Localization. *IEEE Transactions on Robotics and Automation*, 20(4):668–676, 2004.

[Zhang and Pless, 2004] Qilong Zhang and Robert Pless. Extrinsic Calibration for a Camera and Laser Ranger Finder (improves camera intrinsic claibration). In *IEEE/RSJ International Workshop on Intelligent Robots and Systems*, Japan, 2004. IEEE.